Gaussian Radial Growth

Kristjana Ýr Jónsdóttir and Eva B. Vedel Jensen

04

Gaussian Radial Growth

GAUSSIAN RADIAL GROWTH

Kristjana Ýr Jónsdóttir and Eva B. Vedel Jensen

University of Aarhus, Department of Mathematical Sciences,
Ny Munkegade, DK-8000 Aarhus C, Denmark
kyj@imf.au.dk, eva@imf.au.dk

Abstract

The growth of planar and spatial objects is often modelled using one-dimensional size parameters, e.g. volume, area or average radius. We take a more detailed approach and model how the boundary of a growing object expands in time. We mainly consider star-shaped planar objects. The model can be regarded as a dynamic deformable template model. The limiting shape of the object may be circular but this is only one possibility among a range of limiting shapes. An application to tumour growth is presented. Two extensions of the model, involving time series and Lévy bases, respectively, are briefly touched upon.

1. Introduction

Modelling of biological growth patterns is a rapidly developing field of mathematical biology. Its state-of-the-art was explored at the successful conference *On Growth and Form*, held in 1998 in honour of D'Arcy Thompson (1860-1948) and his famous book, cf. Thompson (1917). Out of the conference grew a monograph which contains substantial biological material and an overview of mathematical modelling of spatio-temporal systems, cf. Chaplain et al. (1999). Examples of growth mechanisms studied are growth of capillary networks, skeletal growth and tumour growth.

Modelling of tumour growth has attracted particular interest in recent years. Tumour growth was one of the high priority topics of the recent multidisciplinary conference arranged by the European Society for Mathematical and Theoretical Biology in July 2002. More than 500 scientists from a wide range of disciplines participated. One of the subjects discussed were pattern formation problems, relating to tumour formation and progression, in particular the question of tumour shape.

The models suggested for tumour growth are either continuous or discrete. In Murray (2003), the continuous approach is explained in relation to brain tumours. The simplest models involve only total number of cells in the tumour, with growth of the tumour usually assumed to be exponential, Gompertzian or logistic (Swan (1987), Marusic et al. (1994)). More powerful deterministic models describe the change of the spatial arrangement of the cells under tumour growth. A simple continuous model of this type predicts that the

concentration of cells at position x and time t is

$$c(x,t) = \frac{c}{t} \exp\left(\rho t - \frac{||x||^2}{Dt}\right)$$

where ρ is the net growth rate of cells, including proliferation and death (or loss) and D is the diffusion coefficient. This more realistic model has been used to make prediction of the time evolution of one-dimensional quantities related to growth from which the model parameters can be estimated from experimental data. See also the work by Byrne (1999) and references therein. The discrete models are most often cellular automaton models, cf. Qi et al. (1993), Kansal et al. (2000).

The growth literature contains very few examples of statistical modelling and analysis of growth patterns. An exception is the paper by Cressie and Hulting (1992). Growth of a planar star-shaped object is here modelled, using a sequence of Boolean models. The object Y_{t+1} at time $t + 1$ is the union of independent random compact sets placed at uniform random positions inside the object Y_t at time t. More formally,

$$Y_{t+1} = \cup\{Z(x_i) : x_i \in Y_t\},$$

where $\{x_i\}$ is a homogeneous Poisson point process in the plane and $Z(x_i)$ is a random compact set with position x_i. Note that this model is Markov since Y_{t+1} only depends on the previous objects via Y_t. The model is applied to describe the growth pattern of human breast cancer cell islands. Practical methods of estimating the model parameters, using the information of the complete growth pattern, are devised. A related continuous model has recently been discussed in Deijfen (2003). The object Y_t is here a connected union of randomly sized Euclidean balls, emerging at exponentially distributed times. It is shown that the asymptotic shape is spherical.

In the present paper, we propose a Gaussian radial growth model for star-shaped planar objects. The model is a dynamic version of the $p-$order shape model introduced in Hobolth et al. (2003). The object at time $t + 1$ is a stochastic transformation of the object at time t such that the radius vector function of the object fulfils

$$R_{t+1}(\theta) = R_t(\theta) + Z_t(\theta), \quad \theta \in [0, 2\pi),$$

where Z_t is a cyclic Gaussian process. The coefficients of the Fourier series of Z_t

$$Z_t(\theta) = \mu_t + \sum_{k=1}^{\infty}[A_{t,k}\cos(k\theta) + B_{t,k}\sin(k\theta)], \quad \theta \in [0, 2\pi), \tag{1}$$

have important geometric interpretations relating to the growth process. The overall growth from time t to $t + 1$ is determined by the parameter μ_t. The coefficients $A_{t,1}$ and $B_{t,1}$ determine the asymmetry of growth from time t to $t + 1$, while $A_{t,k}$ and $B_{t,k}$ affect how the growth appears globally for small $k \geq 2$ and locally for large $k \geq 2$. Under the proposed p-order growth model

$$A_{t,k} \sim B_{t,k} \sim N(0, \lambda_{t,k}), \quad k = 2, 3, \ldots,$$

where the variances satisfy the following regression model

$$\lambda_{t,k}^{-1} = \alpha_t + \beta_t(k^{2p} - 2^{2p}), \quad k = 2, 3, \ldots.$$

In Section 2 we introduce the Gaussian radial growth model. In Section 3, we study the induced distributions of object size and shape under the model. An application to tumour growth is discussed in Section 4. Two extensions of the model, involving time series and Lévy bases, respectively, are briefly described in Sections 5 and 6. A 3D version of the Gaussian radial growth model is presented in an Appendix.

2

2. The Gaussian radial growth model

Consider a planar compact object with size and shape changing over time. The object at time t is denoted by $Y_t \subset \mathbb{R}^2$. We suppose that Y_t is star-shaped with respect to a point $z \in \mathbb{R}^2$ for all t. Then, the boundary of Y_t can be determined by its radius vector function $R_t = \{R_t(\theta) : \theta \in [0, 2\pi)\}$ with respect to z, where

$$R_t(\theta) = \max\{r : z + r(\cos\theta, \sin\theta) \in Y_t\}, \quad \theta \in [0, 2\pi).$$

In Hobolth et al. (2003), a deformable template model is introduced, describing a random planar object as a stochastic deformation of a known star-shaped template, see also the closely related models described in Hobolth and Jensen (2000), Kent et al. (2000) and Hobolth et al. (2002). We use this approach here and describe the object at time $t + 1$ as a stochastic transformation of the object at time t, such that

$$R_{t+1}(\theta) = R_t(\theta) + Z_t(\theta), \quad \theta \in [0, 2\pi). \tag{2}$$

Here, $\{Z_t\}$ is a series of independent stationary cyclic Gaussian processes with Z_t short for $\{Z_t(\theta) : \theta \in [0, 2\pi)\}$. The initial value R_0 of the radius vector function is assumed to be known.

Note that Y_t is used as a template in the stochastic transformation, resulting in Y_{t+1}. The increment process Z_t can be written as

$$Z_t(\theta) = \mu_t + U_t(\theta), \quad \theta \in [0, 2\pi),$$

where $\mu_t \in \mathbb{R}$ represents a constant radial addition and U_t a stochastic deformation with mean zero of the expanded object with radius vector function $R_t + \mu_t$, cf. Figure 1. (The object with radius vector function $R_t + \mu_t$ is in geometric tomography known as the radial sum of Y_t and a circular disc of radius μ_t, cf. Gardner (1995).) Because of the independence
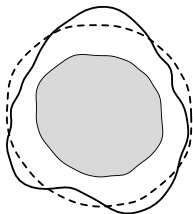

Figure 1: The object Y_{t+1} is a stochastic transformation of the object Y_t (grey), using a constant radial addition (shown stippled) followed by a deformation.

of the Z_ts, the model is Markov in the sense that it uses information about the object at the immediate past to describe the object at the present time. More specifically, under (2) the conditional distribution of R_{t+1} given $R_t, \ldots, R_0$ only depend on R_t. The model suggested in Cressie and Hulting (1992) possesses a similar Markov property.

If Y_t is non-circular, it can be natural to extend the model (2), using an increasing time change function $\Gamma_t : [0, 2\pi] \to [0, 1]$ such that $Z_t \circ \Gamma_t^{-1}$ is stationary. If the boundary length of Y_t is finite, one possibility is to choose

$$\Gamma_t(\theta) = \frac{L_t(\theta)}{L_t(2\pi)}, \tag{3}$$

where $L_t(\theta)$ is the distance travelled along the boundary of Y_t between the points indexed by 0 and θ. Note, however, that if $R_0 \equiv 0$, then the boundary of Y_t is expected to be approximately circular, since $\mathbb{E}(Z_t(\theta))$ does not depend on $\theta \in [0, 2\pi)$.

The following result is important for the construction of parametric models in the framework of model (2). The result also implies a simple simulation procedure for a stationary cyclic Gaussian process on $[0, 2\pi)$.

Proposition 2.1 The process Z_t is a stationary cyclic Gaussian process on $[0, 2\pi)$ with mean $\mu_t \in \mathbb{R}$ if and only if there exist $\lambda_{t,k} \geq 0, k \in \mathbb{N}_0$, such that $\sum_{k=0}^{\infty} \lambda_{t,k} < \infty$ and

$$Z_t(\theta) = A_{t,0} + \sum_{k=1}^{\infty} [A_{t,k} \cos(k\theta) + B_{t,k} \sin(k\theta)], \quad \theta \in [0, 2\pi),$$

where $A_{t,0}, A_{t,k}, B_{t,k}, k = 1, 2, \ldots$, are all independent, $A_{t,0} \sim N(\mu_t, \lambda_{t,0})$ and $A_{t,k} \sim B_{t,k} \sim N(0, \lambda_{t,k})$.

The Fourier coefficients

$$
\begin{aligned}
A_{t,0} &= \frac{1}{2\pi} \int_0^{2\pi} Z_t(\theta) \, d\theta, \\
A_{t,k} &= \frac{1}{\pi} \int_0^{2\pi} Z_t(\theta) \cos(k\theta) \, d\theta, \quad k = 1, 2, \ldots \\
B_{t,k} &= \frac{1}{\pi} \int_0^{2\pi} Z_t(\theta) \sin(\theta k) \, d\theta, \quad k = 1, 2, \ldots
\end{aligned}
\tag{4}
$$

have interesting geometric interpretations relating to the growth process. It is clear that the coefficient $A_{t,0}$ determines the overall growth from Y_t to Y_{t+1}. The Fourier coefficients $A_{t,1}$ and $B_{t,1}$ play also a special role. Numerically large values of the coefficients will imply an asymmetric growth from Y_t to Y_{t+1}. In order to interpret geometrically the remaining Fourier coefficients $A_{t,k}$ and $B_{t,k}$, $k = 2, 3, \ldots$, let us consider an increment process for which all Fourier coefficients except those of order 0 and k are zero,

$$Z_t(\theta) = A_{t,0} + A_{t,k} \cos(k\theta) + B_{t,k} \sin(k\theta), \quad \theta \in [0, 2\pi).$$

Such a process exhibits k-fold symmetry, i.e.

$$Z_t\left(\theta + \frac{2\pi i}{k}\right), \quad i = 0, 1, \ldots, k-1, \quad \theta \in [0, 2\pi),$$

does not depend on i. Therefore, $A_{t,k}$ and $B_{t,k}$ affect how the growth appears globally for small k and locally for large k. The variances $\lambda_{t,k}$ control the magnitude of the Fourier coefficients.

Since the zero- and first-order Fourier coefficients play a special role in relation to the growth process and may in applications well depend on explanatory variables, we shall desist from specific modelling of these coefficients. In the following we will assume that $A_{t,0} = \mu_t$ is deterministic. Furthermore, we suppose that $A_{t,1} = B_{t,1} = 0$ or, equivalently, we concentrate on modelling

$$Z_t(\theta) - A_{t,1} \cos \theta - B_{t,1} \sin \theta, \quad \theta \in [0, 2\pi).$$

A special case of the Gaussian radial growth model is the p-order growth model. This model is inspired by the p-order model described in Hobolth et al. (2003), where the

stochastic deformation process is a stationary Gaussian process with an attractive covariance structure. The model is called p-order because it can be derived as a limit of discrete p-order Markov models defined on a finite, systematic set of angles θ, cf. Hobolth et al. (2002).

Definition 2.2 A stochastic process $Y = \{Y(\theta) : \theta \in [0, 2\pi)\}$ follows a *p-order model*, if

$$Y(\theta) = \mu + \sum_{k=2}^{\infty}[A_k \cos(k\theta) + B_k \sin(k\theta)], \quad \theta \in [0, 2\pi),$$

where $A_k \sim B_k \sim N(0, \lambda_k)$ are all independent and

$$\lambda_k^{-1} = \alpha + \beta(k^{2p} - 2^{2p}), \quad k = 2, 3, \ldots.$$

The parameters satisfy $\mu \in \mathbb{R}$, $\alpha, \beta > 0$ and $p > \frac{1}{2}$.

If Y follows a $p-$order model, we will write $Y \sim G_p(\mu, \alpha, \beta)$. Clearly, μ is the mean of Y. Furthermore, the covariance function of Y is of the form

$$\sigma(\theta) = \text{Cov}(Y(0), Y(\theta)) = \sum_{k=2}^{\infty} \lambda_k \cos(k\theta) = \sum_{k=2}^{\infty} \frac{\cos(k\theta)}{\alpha + \beta(k^{2p} - 2^{2p})},$$

$\theta \in [0, 2\pi)$. The parameters α and β determine the variance of lower order and higher order Fourier coefficients, respectively. Furthermore, p determines the smoothness of the curve Y. In fact, the curve Y is $k - 1$ times continuously differentiable where k is the unique integer satisfying $p \in (k - \frac{1}{2}, k + \frac{1}{2}]$ (Hobolth et al. (2003)). Note that the first Fourier coefficients of Y are set to zero.

We can now give the definition of the $p-$order growth model.

Definition 2.3 The series $Z = \{Z_t\}$ follows a $p-$order growth model if the Z_ts are independent and $Z_t \sim G_p(\mu_t, \alpha_t, \beta_t)$ for all t.

The parameters α_t and β_t determine, respectively, the global and local appearance of growth from Y_t to Y_{t+1}. As before, p determines the smoothness of the curves Z_t. The overall growth pattern is specified by the μ_ts. Their actual form depends on the specific application. Tumour growth has often been described by a Gompertz growth pattern

$$\rho_t = \rho_0 \exp\left[\frac{\eta}{\gamma}(1 - \exp(-\gamma t))\right],$$

where ρ_t is the average radius at time t and η and γ are positive parameters determining the growth, implying that

$$\mu_t = \rho_t\left(\exp\left[\frac{\eta}{\gamma}\exp(-\gamma t)(1 - \exp(-\gamma))\right] - 1\right).$$

For more details, see e.g. Steel (1977).

Figure 2 shows simulations of the increment process Z_t from time t to $t+1$ for different values of α_t and β_t under the second-order growth model. A large value of α_t gives increments that are fairly constant while a small value of α_t provides a more irregular growth on a global scale. The parameter β_t controls the local appearance of the increment process, the smaller β_t the more pronounced irregularity on a local scale.
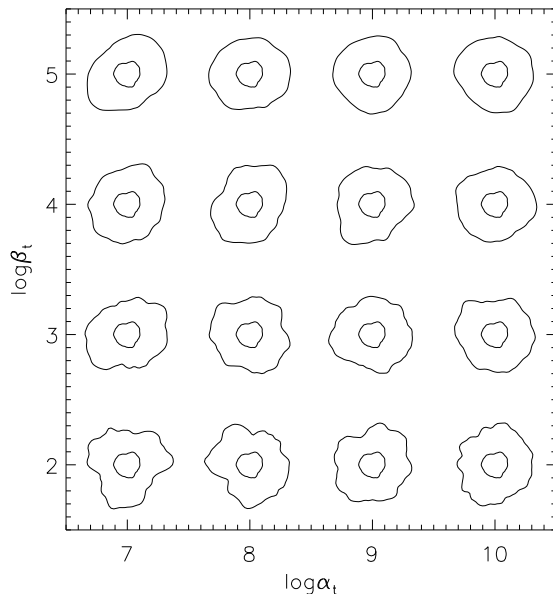
5

Figure 2: Simulated objects under the second-order growth model. The object at time t is fixed while the object at time $t+1$ is simulated under the indicated values of α_t and β_t.

3. Distributional results

In this section, we study the induced distribution of object size and shape under the p-order growth model. The limiting shape may be circular but, as we shall see, there is a whole range of possibilities.

Unless otherwise explicitly stated, we assume that $R_0 \equiv 0$. We then have for $\theta \in [0, 2\pi)$

$$R_T(\theta) = \rho_T + \sum_{k=2}^{\infty}[A_k^T \cos(k\theta) + B_k^T \sin(k\theta)], \tag{5}$$

where $A_k^T \sim B_k^T \sim N(0, \lambda_k^T)$ are all independent,

$$\rho_T = \sum_{t=0}^{T-1} \mu_t, \tag{6}$$

and

$$\lambda_k^T = \sum_{t=0}^{T-1} \lambda_{t,k}. \tag{7}$$

The shape of the object at time T will be represented by its normalized radius vector function

$$\frac{R_T}{\mathbb{E}(R_T(0))} = \frac{R_T}{\rho_T},$$

which can be regarded as a continuous analogue of the standardized vertex transformation vector in shape theory, cf. Hobolth et al. (2002).

Under the assumption of independent increments, the distribution of the area of the object at time T is known.

6

Proposition 3.1 Let the radius vector function R_T of the object Y_T at time T satisfy (5)–(7). Then,

$$\mathrm{A}(Y_T) \sim \pi\rho_T^2 + \frac{\pi}{2}\sum_{k=2}^{\infty}\lambda_k^T V_k,$$

where V_k, $k = 2, 3, \ldots$, are mutually independent $\chi^2(2)$-distributed random variables.

Proof. The area of the object at time T is

$$\mathrm{A}(Y_T) = \frac{1}{2}\int_0^{2\pi} R_T(\theta)^2 \mathrm{d}\theta.$$

Note that since

$$\sum_{k=2}^{\infty}(A_k^T)^2 + (B_k^T)^2 < \infty, \ \ \mathbb{P}\text{-a.s.},$$

we have that $R_T \in L_2([0, 2\pi])$, $\mathbb{P}$-a.s. Using equation (5) and Parseval's equation, we get that

$$\mathrm{A}(Y_T) = \pi\rho_T^2 + \frac{\pi}{2}\sum_{k=2}^{\infty}[(A_k^T)^2 + (B_k^T)^2]$$

$$= \pi\rho_T^2 + \frac{\pi}{2}\sum_{k=2}^{\infty}\lambda_k^T V_k,$$

where V_k, $k = 2, 3, \ldots$, are mutually independent $\chi^2(2)$-distributed random variables. $\square$

The distribution of the area of Y_T is thus a sum of independent Gamma distributed random variables. The saddlepoint approximation of such a distribution is easily derived, cf. Jensen (1992).

It does not seem possible to get a correspondingly simple result for the distribution of the boundary length of Y_T. This seems apparent from the expression for the boundary length of Y_T

$$\int_0^{2\pi}\sqrt{R_T'(\theta)^2 + R_T(\theta)^2}d\theta,$$

which is valid in the case where R_T is differentiable.

As we shall see now, the class of p-order growth models is quite rich in the sense that the shape of the limiting object, represented by its normalized radius vector function, may be distributed according to any p-order model $G_p(1, \alpha, \beta)$ with mean 1. For large values of α and β, the shape is close to circular.

Let us consider the p-order growth model with proportional parameters, i.e. $\alpha_t = \gamma\beta_t$. Equivalently, we assume that there exists a sequence $\{\tau_t\}$ of positive real numbers such that

$$Z_t = \mu_t + \tau_t X_t \tag{8}$$

and $\{X_t\}$ are independent and identically $G_p(0, \alpha, \beta)$ distributed. If $\sigma^2 = \mathbb{V}(X_t(\theta))$, then $Z_t(\theta) \sim N(\mu_t, \tau_t^2\sigma^2)$ under (8).

Examples of choices of τ_t are $\tau_t = 1$, $\sqrt{\mu_t}$ or ρ_{t+1}, cf. (6). If $\tau_t = 1$, the variance of the increment $Z_t(\theta)$ is constant in time. If $\tau_t = \sqrt{\mu_t}$, we obviously need that $\mu_t \geq 0$ for all t and we have that $\mathbb{V}(Z_t(\theta)) \propto \mathbb{E}(Z_t(\theta))$ such that the variance of the increment $Z_t(\theta)$ is proportional to the average increase in the radius at time t. If $\tau_t = \rho_{t+1}$, then the distribution of the shape of the object defined by the radius vector function

$$\{\rho_t + Z_t(\theta): \quad \theta \in [0, 2\pi]\}$$

is constant in time, i.e. the distribution of

$$\frac{\rho_t + Z_t(\theta)}{\mathbb{E}(\rho_t + Z_t(\theta))}$$

does not depend on t.

In the proposition below, we show that under (8) the shape of Y_t is distributed according to a p-order model.

Proposition 3.2 Suppose that $Z = \{Z_t\}$ satisfies (8) where $X_t, t \in \mathbb{N}_0$, are independent and identically $G_p(0, \alpha, \beta)-$distributed. Then, the normalized radius vector function of Y_T is distributed as

$$\frac{R_T}{\mathbb{E}(R_T(0))} \sim G_p(1, \bar{\alpha}_T, \bar{\beta}_T)$$

where

$$\bar{\alpha}_T = \alpha \rho_T^2 / \sum_{t=0}^{T-1} \tau_t^2, \quad \bar{\beta}_T = \beta \rho_T^2 / \sum_{t=0}^{T-1} \tau_t^2.$$

Proof. It suffices to show that

$$\frac{\text{Cov}(R_T(0), R_T(\theta))}{[\mathbb{E}(R_T(0)]^2} = \sum_{k=2}^{\infty} \frac{\cos(k\theta)}{\bar{\alpha}_T + \bar{\beta}_T(k^{2p} - 2^{2p})}.$$

Using (5) and (8), we find

$$\frac{\text{Cov}(R_T(0), R_T(\theta))}{[\mathbb{E}(R_T(0)]^2} = \frac{1}{\rho_T^2} \sum_{k=2}^{\infty} \lambda_k^T \cos(k\theta)$$

$$= \frac{1}{\rho_T^2} \sum_{k=2}^{\infty} \sum_{t=0}^{T-1} \tau_t^2 \frac{\cos(k\theta)}{\alpha + \beta(k^{2p} - 2^{2p})}$$

$$= \sum_{k=2}^{\infty} \frac{\cos(k\theta)}{\bar{\alpha}_T + \bar{\beta}_T(k^{2p} - 2^{2p})}.$$

$\square$

Below, we study examples of different limiting shapes under the model (8).

Example 3.3 (Constant increment growth) Let the situation be as in Proposition 3.2 with $\mu_t = \mu$ and $\tau_t = 1$ in (8). The increment processes Z_t are thereby independent and identically distributed. It follows from Proposition 3.2 that

$$\frac{R_T}{\mathbb{E}R_T(0)} \sim G_p(1, \bar{\alpha}_T, \bar{\beta}_T),$$

where $\bar{\alpha}_T = T\mu^2\alpha$ and $\bar{\beta}_T = T\mu^2\beta$. Since $\bar{\alpha}_T \to \infty$ and $\bar{\beta}_T \to \infty$ for $T \to \infty$, the boundary of the object becomes more circular and smooth as T increases. An example is shown in Figure 3. The limiting object has circular shape.

Example 3.4 (Wiener growth) Let the situation be as in Proposition 3.2 with μ_t arbitrary and $\tau_t = \sqrt{\mu_t}$ in (8). This special case is called a Wiener growth model since $\mathbb{V}(R_T) \propto \mathbb{E}(R_T)$. If $\mu_t = \mu$ such that $\rho_T = T\mu$, the process is called a Wiener process with

linear drift. If $\rho_T = \delta T^\psi$ for some $\delta, \psi > 0$, then $R_T - \rho_T$ is self-similar with parameter $H = \frac{\psi}{2}$, i.e.

$$R_{at} - \rho_{at} \sim a^H (R_t - \rho_t), \quad a \geq 0. \tag{9}$$

Notice that

$$\frac{R_T}{\mathbb{E}R_T(0)} \sim G_p(1, \alpha\rho_T, \beta\rho_T).$$

If $\rho_T \to \rho < \infty$, the limiting object can have any stochastic shape determined by $G_p(1, \alpha\rho, \beta\rho)$.

Example 3.5 Let the situation be as in Proposition 3.2 with μ_t arbitrary and $\tau_t = \rho_{t+1}$ in (8). The normalized radius vector function is distributed as

$$\frac{R_T}{\mathbb{E}R_T(0)} \sim G_p(1, \alpha \frac{\rho_T^2}{\sum_{t=1}^T \rho_t^2}, \beta \frac{\rho_T^2}{\sum_{t=1}^T \rho_t^2}).$$

If $\rho_T^2 / \sum_{t=1}^T \rho_t^2 \to 0$ as $T \to \infty$, the objects become more irregular both globally and locally as T increases. An example is shown in Figure 4.
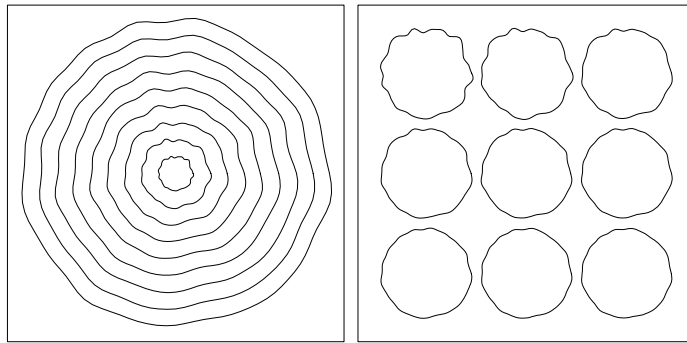

Figure 3: Left: Simulated growth pattern under the constant increment second-order growth model. Right: The corresponding normalized profiles, representing the shape of the object.
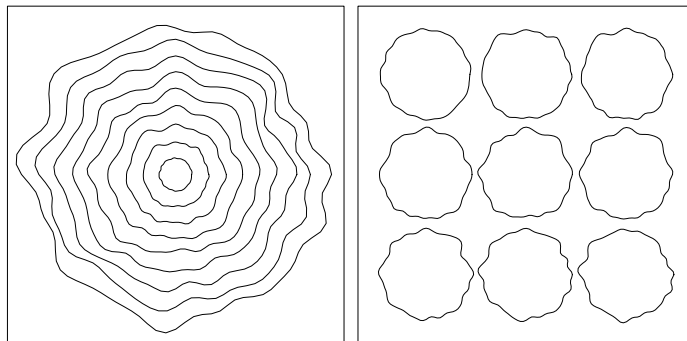

Figure 4: Left: Simulated growth pattern under the model described in Example 3.5. Right: The corresponding normalized profiles, representing the shape of the object.

4. An application

For illustrative purposes, we consider a data set consisting of human breast cancer cell islands, which have been observed in vitro in a nutrient medium on a flat dish. This data set has earlier been analysed in Cressie and Hulting (1992). Three profiles of cancer cell islands are available. The data set is presented in the upper left corner of Figure 5.

Figure 5: The tumour growth data (upper left corner) and simulations under the second-order growth model with μ_t, α_t and β_t replaced by the maximum likelihood estimates.

The centre of mass of Y_0 is used as reference point. The data consist of increments

$$z_t\left(\frac{2\pi i}{n_t}\right), \quad i = 0, 1, \ldots, n_t - 1,$$

in n_t directions, equidistant in angle, $t = 0, 1$. For convenience, z_t is normalized with the average radius of Y_0. Only digitized images are available. As n_t, we have used approximately 25% of the number of pixels on the boundary of the digitized image of Y_t, $t = 0, 1$.

Under the p-order growth model, the mean value parameters μ_t can be estimated by the average observed increment at time t. The variance parameters can be estimated using the likelihood function

$$L(\alpha_0, \beta_0, \alpha_1, \beta_1) = \prod_{t=0,1} L_t(\alpha_t, \beta_t),$$

where $L_t(\alpha_t, \beta_t)$ is the likelihood function based on the Fourier coefficients $A_{t,k}$ and $B_{t,k}$ of Z_t of order $k \leq K_t$, say. Since $A_{t,k} \sim B_{t,k} \sim N(0, \lambda_{t,k})$ are all independent and

$$\lambda_{t,k}^{-1} = \alpha_t + \beta_t(k^{2p} - 2^{2p}), \quad k = 2, 3, \ldots,$$

the likelihood becomes

$$L_t(\alpha_t, \beta_t) = \prod_{k=2}^{K_t} [\alpha_t + \beta_t(k^{2p} - 2^{2p})] \exp(-c_{t,k}[\alpha_t + \beta_t(k^{2p} - 2^{2p})]),$$

where $c_{t,k} = [a_{t,k}^2 + b_{t,k}^2]/2$ are the observed phase amplitudes. In applications, $a_{t,k}$ and $b_{t,k}$ are replaced by discrete versions of the integrals in (4).

The choice of the cut-off value K_t is very important. Clearly, K_t must not be too large in order to avoid that the estimates are influenced by the digitization effects. On the other hand, if the cut-off value K_t is too small information about the growth pattern is

10

lost. The choice of K_t should be an intermediate value for which the estimate of the local parameter β_t is stable. Whether a specific choice of K_t is appropriate can also be judged from visual inspection of simulated growth patterns under the estimated model.

For the two increments z_0 and z_1, we used $(n_0, K_0) = (60, 25)$ and $(n_1, K_1) = (120, 30)$, respectively. The maximum likelihood estimates under the second-order growth model are

$$\hat{\mu}_0 = 1.04, \log(\hat{\alpha}_0) = 5.29, \log(\hat{\beta}_0) = -1.88,$$
$$\hat{\mu}_1 = 2.53, \log(\hat{\alpha}_1) = 3.18, \log(\hat{\beta}_1) = -3.54.$$

The estimated regression lines

$$\hat{\lambda}_{t,k} = \frac{1}{\hat{\alpha}_t + \hat{\beta}_t(k^4 - 2^4)}, \quad t = 0, 1 \quad k = 2, 3, \dots$$

are shown in Figure 6, together with 95% confidence limits for the logarithm of the phase amplitudes. The model fits the data well which can also be seen from the QQ plots for the normalized Fourier coefficients, also shown in Figure 6.
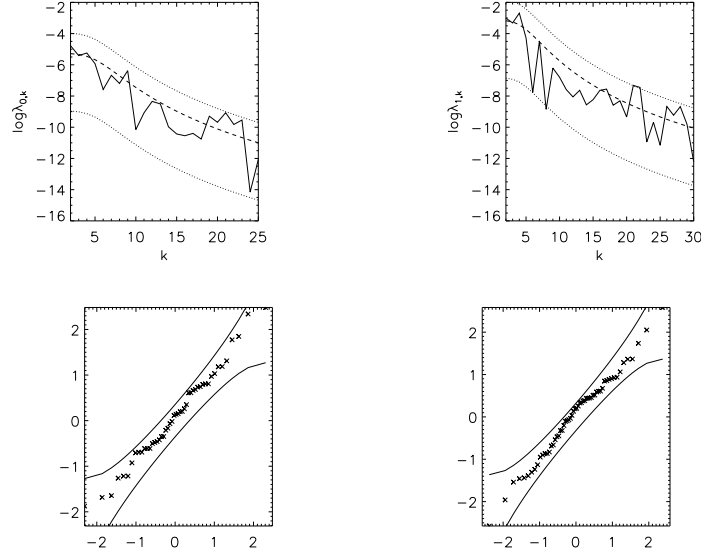

Figure 6: The two upper figures show the observed phase amplitudes (full-drawn lines) together with the estimated regression line (stippled) and 95% confidence limits. The two lower figures show QQ plots for the normalized Fourier coefficients $\frac{a_{t,k}}{\sqrt{\hat{\lambda}_{t,k}}}, \frac{b_{t,k}}{\sqrt{\hat{\lambda}_{t,k}}}$ together with 95% confidence limits.

Simulations under the second-order growth model with μ_t, α_t and β_t replaced by the maximum likelihood estimates are shown in Figure 5.

Since the data set only contains two increments, it is not meaningful to try to evaluate the Markov assumption. Note also that the Z_t's are assumed independent but not necessarily identically distributed. If

$$\alpha_t = \gamma\beta_t, \tag{10}$$

we have that

$$\sqrt{\beta_t}(Z_t - \mu_t) \sim G_p(0, \gamma, 1)$$

11

are independent and identically distributed. Thus, under the assumption (10) of proportionality and with sufficient number T of time points, we can examine the independence of

$$\sqrt{\beta_t}(Z_t(\theta) - \mu_t), \quad t = 0, 1, \ldots, T - 1,$$

for selected values of $\theta \in [0, 2\pi)$, using a runs test, for instance.

5. A time series extension

Let us suppose that

$$Z_t = \mu_t + \tau_t X_t,$$

where $X = \{X_t\}$ is a stationary time series of cyclic Gaussian processes satisfying the ARMA model equation

$$X_t - \phi_1 X_{t-1} - \cdots - \phi_r X_{t-r} = W_t - \psi_1 W_{t-1} - \cdots - \psi_s W_{t-s}. \tag{11}$$

We assume that $W = \{W_t\}$ is a sequence of i.i.d. stationary cyclic Gaussian processes on $[0, 2\pi)$ with

$$W_t \sim G_p(0, \alpha, \beta).$$

If $\phi_i = 0$, $i = 1, \ldots, r$, and $\psi_j = 0$, $j = 1, \ldots, s$, Z follows the p-order growth model with independent increments, treated in the previous sections.

Under the general ARMA model (11), the Fourier coefficients of X and W of a given order follow a one-dimensional ARMA model. Furthermore, for fixed $\theta \in [0, 2\pi)$, $X_t(\theta)$ follows a one-dimensional ARMA model. Aspects of this time series approach has earlier been discussed in Alt (1999). An early example concerning year ring widths is discussed in Kronborg (1981).

Note that in the special case of a MA model ($\phi_1 = \cdots = \phi_r = 0$), the marginal distribution of Z_t belongs to the class of p-order models

$$Z_t \sim G_p(\mu_t, \alpha_t, \beta_t),$$

where

$$\alpha_t = \frac{\alpha}{\tau_t^2[1 + \psi_1^2 + \cdots + \psi_s^2]}, \quad \beta_t = \frac{\beta}{\tau_t^2[1 + \psi_1^2 + \cdots + \psi_s^2]}.$$

Note also that in this case Z_t and $Z_{t'}$ are independent if $|t - t'| > s$.

6. A Lévy based extension

Following the approach in Barndorff-Nielsen and Schmiegel (2003), let $\mathcal{P} = [0, 2\pi) \times \mathbb{R}$ and $\mathcal{B} = \mathcal{B}(\mathcal{P})$, and consider the following model equation

$$R_{t+1}(\theta) = R_t(\theta) + Z_t(\theta), \quad \theta \in [0, 2\pi) \tag{12}$$

where

$$Z_t(\theta) = \int_{A_t(\theta)} h_t(a; \theta) Z(da), \tag{13}$$

$A_t(\theta) \in \mathcal{B}$ and Z is a normal Lévy basis on $\mathcal{P}$. In particular, for a bounded set $A \in \mathcal{B}$,

$$Z(A) \sim N(\nu(A)\mu, \nu(A)\sigma^2),$$

where ν is the Lebesgue measure on $\mathcal{P}$. The so-called ambit set $A_t(\theta)$ and the weight function $h_t(a;\theta)$ must be defined cyclically such that Z_t becomes a cyclic stochastic process. Also, $h_t(a;\theta)$ is assumed to be suitable for the integral to exist.

Since

$$\mathrm{Cov}(Z_t(\theta_1), Z_{t'}(\theta_2)) = \sigma^2 \int_{A_t(\theta_1) \cap A_{t'}(\theta_2)} h_t(a;\theta_1) h_{t'}(a;\theta_2)\, da,$$

the ambit sets $A_t(\theta)$ and the weight functions $h_t(\cdot;\theta)$ determine the correlation structure of the increment processes $\{Z_t\}$. Note that if

$$A_t(\theta_1) \cap A_{t'}(\theta_2) = \emptyset,$$

then Z_t and $Z_{t'}$ are independent. Note also that asymmetric growth patterns are generated if the weight function $h_t(\cdot;\theta)$ or the ambit set $A_t(\theta)$ depend on the angle θ.

The model specification (13) is attractive because both the angular and temporal correlations of the increment processes can be expressed explicitly. The question is now whether it is possible to specify A_t and h_t such that Z_t follows a $p-$order model. In the appendix, we show that a first-order model is attainable within this framework. The general question remains open.

7. Discussion

The $p-$order growth model has mainly been suggested as a general tool for analyzing observed radial growth patterns. The model may, however, also be of interest as a building block in other modelling situations, for instance in models for tessellations where cells are created by radial growth from each point of a point process.

The $p-$order growth model can be extended in various ways. It is obviously easy to modify the model such that the increments are Gaussian after a transformation. An example is log-Gaussian increments. If the number of increments observed is not too small it is also of interest to try to model the dependency in the series $Z = \{Z_t\}$. We have looked at time series and Lévy based models. A detailed study of the Lévy based growth models with not necessarily normal Lévy bases is ongoing research in our group, cf. Schmiegel et al. (2004). These models can be formulated continuously in time

$$R_t(\theta) = r_0(\theta) + \int_0^t Z_s(\theta)\, ds,$$

where r_0 is a deterministic function.

The likelihood used in the application is correct if the increments are independent. If the marginal distributions of the Z_ts belong to the class of p-order models but the Z_ts are dependent, the likelihood may still be used as a pseudo-likelihood.

In relation to tumour growth in particular, it will also be of interest in the future to try to embed specific mathematical models in a stochastic framework. A starting point could here be a study of dynamic point process models with a specified time-dependent intensity function. One example of such an intensity function is given in the introduction.

8. Acknowledgements

Appendix

A Lévy based extension
In the following, we will show that a first-order model for Z_t can be obtained within the Lévy based framework (12) and (13). We will here represent functions on $[-\pi, \pi)$ rather than on $[0, 2\pi)$.

Let us assume that $h_t \equiv 1$, such that $Z_t(\theta) = Z(A_t(\theta))$ and

$$\text{Cov}(Z_t(\theta_1), Z_t(\theta_2)) = \sigma^2 \nu(A_t(\theta_1) \cap A_t(\theta_2)), \tag{14}$$

where ν denotes Lebesgue measure. Also assume that the ambit sets are on the following form

$$A_t(\theta) = (\theta, 0) + A_t(0), \quad \theta \in [-\pi, \pi),$$

with a cyclic definition in the angle θ. Furthermore, let us suppose that there exists a continuous function f_t on $[-\pi, \pi)$ with the properties

$$f_t(\theta) = f_t(-\theta) \tag{15}$$
$$f_t \text{ is decreasing on } [0, \pi) \tag{16}$$
$$f_t(0) = t \tag{17}$$

such that

$$A_t(0) = \{(\theta', t') : f_t(\pi) \leq t' \leq f_t(\theta')\}. \tag{18}$$

Note that Z_{t-1} and Z_t are independent if $t - 1 < f_t(\pi)$.

It is not difficult to show that

$$\nu(A_t(0) \cap A_t(\theta)) = 2 \int_{-\pi}^{-\pi + \frac{\theta}{2}} f_t(\phi) \, d\phi + 2 \int_{\frac{\theta}{2}}^{\pi} f_t(\phi) \, d\phi - 2\pi f_t(\pi), \tag{19}$$

for $\theta \in [0, \pi)$. Furthermore, since

$$\nu(A_t(0) \cap A_t(-\theta)) = \nu(A_t(0) \cap A_t(\theta)), \tag{20}$$

the Fourier expansion of the intersection areas are of the form

$$\nu(A_t(0) \cap A_t(\theta)) = \sum_{k=0}^{\infty} \lambda_{t,k} \cos(k\theta). \tag{21}$$

In a similar way,

$$f_t(\theta) = \sum_{k=0}^{\infty} \gamma_{t,k} \cos(k\theta). \tag{22}$$

Using equations (19) and (22), we find the following alternative expression for the intersection areas

$$\nu(A_t(0) \cap A_t(\theta)) = -4 \, \text{sign}(\theta) \sum_{k \text{ odd}} \frac{\gamma_{t,k}}{k} \sin\left(k\frac{\theta}{2}\right) + 2\pi \sum_{k \text{ odd}} \gamma_{t,k} - 2\pi \sum_{k \text{ even}} \gamma_{t,k}. \tag{23}$$

Comparing the Fourier expansions (21) and (23) we get the following relation between the $\lambda_{t,k}$s and $\gamma_{t,k}$s,

$$\lambda_{t,0} = \sum_{k \text{ odd}} \left[2\pi - \frac{8}{\pi k^2} \right] \gamma_{t,k} - 2\pi \sum_{k \text{ even}} \gamma_{t,k}$$

$$\lambda_{t,j} = \frac{16}{\pi} \sum_{k \text{ odd}} \frac{1}{(2j)^2 - k^2} \gamma_{t,k}, \quad j = 1, 2, \dots.$$

Now consider a model where the functions f_t defining the ambit sets are of the form

$$f_t(\theta) = \gamma_{t,0} + \gamma_{t,1} \cos(\theta).$$

In this case we have the following restrictions on the parameters $\gamma_{t,0}$ and $\gamma_{t,1}$

$$\gamma_{t,0} + \gamma_{t,1} = t, \quad \gamma_{t,1} \geq 0.$$

We find

$$\lambda_{t,0} = \left[2\pi - \frac{8}{\pi} \right] \gamma_{t,1} - 2\pi \gamma_{t,0}$$

$$\lambda_{t,j} = \frac{16}{\pi} \frac{1}{(2j)^2 - 1} \gamma_{t,1}, \quad j = 1, 2, \dots.$$

It follows that Z_t is distributed according to a first-order model.

Extension to three dimensions

The p-order growth model for planar objects can easily be extended to three dimensions. Consider a spatial compact object $Y_t \subset \mathbb{R}^3$ which is star-shaped for all t with respect to $z \in \mathbb{R}^3$. Clearly the boundary of the object can be determined by

$$\{ z + R_t(\theta, \varphi) : \quad \theta \in [0, 2\pi), \quad \varphi \in [0, \pi] \},$$

where $R_t(\theta, \varphi)$ is the distance from z to the boundary of Y_t in direction

$$\omega(\theta, \varphi) = (\sin \varphi \cos \theta, \sin \varphi \sin \theta, \cos \varphi).$$

In the same way as in the planar case we let the object Y_{t+1} be a stochastic transformation of the object Y_t, such that

$$R_{t+1}(\theta, \varphi) = R_t(\theta, \varphi) + Z_t(\theta, \varphi), \quad \theta \in [0, 2\pi), \quad \varphi \in [0, \pi],$$

where $\{ Z_t \}$ is a time series of Gaussian procesess on $[0, 2\pi) \times [0, \pi]$. Writing the stochastic process Z_t in terms of its Fourier-Legendre series expansion we get, cf. Hobolth (2003),

$$Z_t(\theta, \varphi) = \sum_{n=0}^{\infty} \sum_{m=-n}^{m=n} A_{t,n,m} \phi_{n,m}(\theta, \varphi),$$

where $\phi_{n,m}$ are the spherical harmonics and $A_{t,n,m}$ are random coefficients. Using a similar reasoning as in Hobolth (2003) it can be seen that $A_{t,0,0}$ determines the overall growth from Y_t to Y_{t+1}. The coefficients $A_{t,1,m}$, $m = -1, 0, 1$, control the asymmetry of growth, and the remaining coefficients $A_{t,n,m}$ for $n \geq 2$, $m = -n, \dots, n$, affect how the growth appears globally for small n and locally for large n. A p-order growth model can be defined by assuming that $A_{t,0,0} = \mu_t$, $A_{t,1,m} = 0$ for $m = -1, 0, 1$ and

$$A_{t,n,m} \sim N(0, \lambda_{t,n}), \quad n = 2, 3, \dots, m = -n, \dots, n, \text{ independent,}$$

where
$$\lambda_{t,n}^{-1} = \alpha_t + \beta_t(n^{2p} - 2^{2p}).$$

As in the planar case, the increment processes may be chosen to be normal after a transformation. A simulation from such a model, where $\{Z_t\}$ is a series of log-Gaussian processes, is shown in Figure 7.
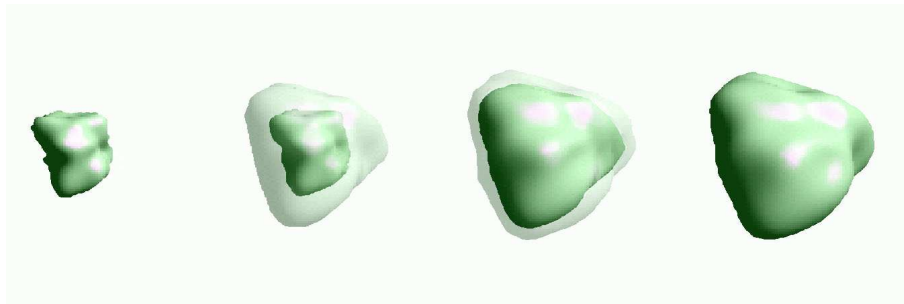

Figure 7: Simulation from a 3D log-Gaussian radial growth model.

References

Alt, W. (1999). Statistics and dynamics of cellular shape changes. In Chaplain, M. A. J., Singh, G. D., and McLachlan, J. C., editors, *On Growth and Form: Spatio-temporal Pattern Formation in Biology*, pages 287–307. Wiley, Chichester.

Barndorff-Nielsen, O. and Schmiegel, J. (2003). Lévy based tempo-spatial modelling; with applications to turbulence. Technical report, MaPhySto Research Report no. 20, University of Aarhus. To appear in Proceedings of the Conference "Kolomogorov and Contemporary Mathematics", held at Moscow State University, 16-21 June 2003.

Byrne, H. (1999). Using mathematics to study solid tumour growth. Proceedings of the 9th general meeting of European women in mathematics.

Chaplain, M. A. J., Singh, G. D., and McLachlan, J. C. (1999). *On Growth and Form: Spatio-temporal Pattern Formation in Biology*. Wiley, Chichester.

Cressie, N. and Hulting, F. L. (1992). A spatial statistical analysis of tumor growth. *J. Amer. Statist. Assoc.*, 87:272–283.

Deijfen, M. (2003). Asymptotic shape in a continuum growth model. *Advances in Applied Probability (SGSA)*, 35:303–318.

Gardner, R. (1995). *Geometric Tomography*. Cambridge University Press, New York.

Hobolth, A. (2003). The spherical deformation model. *Biostatistics*, 4:583–595.

Hobolth, A. and Jensen, E. (2000). Modelling stochastic changes in curve shape, with an application to cancer diagnostics. *Advances in Applied Probability (SGSA)*, 32:344–362.

Hobolth, A., Kent, J., and Dryden, I. (2002). On the relation between edge and vertex modelling in shape analysis. *Scandinavian Journal of Statistics*, 29:355–374.

Hobolth, A., Pedersen, J., and Jensen, E. B. V. (2003). A continuous parametric shape model. *Ann. Inst. Statist. Math.*, 55:227–242.

Jensen, J. (1992). A note on a conjecture of H.E. Daniels. *Revista Brasileira de Probabilidade e Estatística*, 6:85–95.

Kansal, A. R., Torquato, S., Harsh, G. R., Chiocca, E. A., and Deisboeck, T. S. (2000). Simulated brain tumor growth dynamics using a three-dimensional cellular automaton. *J. Theor. Biol.*, 203:367–382.

Kent, J., Dryden, I., and Anderson, C. (2000). Using circulant symmetry to model featureless objects. *Biometrika*, 87:527–544.

Kronborg, D. (1981). Distribution of crosscorrelations in two-dimensional time series, with application to dendrochronology. Research report no. 72, Department of Theoretical Statistics, Institute of Mathematics, University of Aarhus.

Marusic, M., Bajzer, Z., Freyer, J. P., and Vuk-Pavlovic, S. (1994). Analysis of growth of multicellular tumour spheroids by mathematical models. *Cell Prolif.*, 27:73–94.

Murray, J. D. (2003). *Mathematical Biology. II: Spatial Models and Biomedical Applications*. Springer-Verlag, Berlin.

Qi, A.-S., Zheng, X., Du, C.-Y., and Bao-Sheng, A. (1993). A cellular automaton model of cancerous growth. *J. Theor. Biol.*, 161:1–12.

Schmiegel, J., Jónsdóttir, K. Ý., Barndorff-Nielsen, O. E., and Jensen, E. B. V. (2004). Lévy based growth models. In preperation.

Steel, G. G. (1977). *Growth kinetics of tumours*. Clarendon Press, Oxford.

Swan, G. W. (1987). Tumour growth models and cancer therapy. In Thompson, J. R. and Brown, B. R., editors, *Cancer Modeling*, pages 91–104. Marcel Dekker, New York.

Thompson, D. W. (1917). *On Growth and Form*. Cambridge University Press, Cambridge.